Engineering 39 (2024) 204–221

Contents lists available at ScienceDirect

Engineering

journal homepage: www.elsevier.com/locate/eng

Research
Civil Engineering—Article

Lunar *In Situ* Large-Scale Construction: Quantitative Evaluation of Regolith Solidification Techniques

Charun Bao [a], Daobo Zhang [a], Qinyu Wang [a], Yifei Cui [b], Peng Feng [a,*]

[a] MOE Key Laboratory of Civil Engineering Safety and Durability, Department of Civil Engineering, Tsinghua University, Beijing 100084, China
[b] State Key Laboratory of Hydroscience and Engineering, Tsinghua University, Beijing 100084, China

ARTICLE INFO

Article history:
Received 17 October 2023
Revised 22 February 2024
Accepted 5 March 2024
Available online 24 March 2024

Keywords:
Lunar habitats
Lunar *in situ* construction
Regolith bag
Solidification and formation
In situ materials
Evaluation method

ABSTRACT

Lunar habitat construction is crucial for successful lunar exploration missions. Due to the limitations of transportation conditions, extensive global research has been conducted on lunar *in situ* material processing techniques in recent years. The aim of this paper is to provide a comprehensive review, precise classification, and quantitative evaluation of these approaches, focusing specifically on four main approaches: reaction solidification (RS), sintering/melting (SM), bonding solidification (BS), and confinement formation (CF). Eight key indicators have been identified for the construction of low-cost and high-performance systems to assess the feasibility of these methods: *in situ* material ratio, curing temperature, curing time, implementation conditions, compressive strength, tensile strength, curing dimensions, and environmental adaptability. The scoring thresholds are determined by comparing the construction requirements with the actual capabilities. Among the evaluated methods, regolith bagging has emerged as a promising option due to its high *in situ* material ratio, low time requirement, lack of high-temperature requirements, and minimal shortcomings, with only the compressive strength falling below the neutral score. The compressive strength still maintains a value of 2–3 MPa. The proposed construction scheme utilizing regolith bags offers numerous advantages, including rapid and large-scale construction, ensured tensile strength, and reduced reliance on equipment and energy. In this study, guidelines for evaluating regolith solidification techniques are provided, and directions for improvement are offered. The proposed lunar habitat design based on regolith bags is a practical reference for future research.

1. Introduction

As the Earth's closest natural planet, the Moon plays a vital role in human exploration of the universe. Lunar exploration activities began half a century ago, and a resurgence of global interest has occurred in recent years. The growing demand for space activities and remarkable advancements in space technologies have fueled enthusiasm for this research. In 2019, the Artemis Program was proposed for the purpose of establishing a sustainable presence on the lunar surface within the next decade [1]. Moreover, in 2021, China and Russia released a construction plan for the International Lunar Research Station (ILRS) [2,3], outlining a three-step strategy of exploration, construction, and application for the construction of the ILRS. Furthermore, certain space powers, such as Europe, Japan, Republic of Korea, and India, have actively participated in lunar exploration research, launching lunar probes and investigating regolith solidification and formation [4–7]. Lunar construction has become an important engineering requirement and a popular research topic in the field of lunar exploration.

Lunar construction is a complex process that is significantly challenging, requiring comprehensive consideration and integrated design across various aspects, such as architectural form, material preparation, structural layout, and construction technology. Due to the prohibitively high cost and logistical difficulties associated with transporting materials from the Earth to the Moon, engineers and researchers have reached a consensus on the need for *in situ* resource utilization (ISRU), which aims to maximize the utilization of *in situ* construction materials and cooperate with a small amount of external material. Lunar regolith, which are widely distributed and easily accessible on the Moon, serve as abundant and convenient *in situ* resources, rendering them highly suitable for constructing large-scale structures. Considerable

* Corresponding author.
E-mail address: fengpeng@tsinghua.edu.cn (P. Feng).

https://doi.org/10.1016/j.eng.2024.03.004
2095-8099/

theoretical and experimental efforts have been invested in exploring regolith solidification and formation processes. Approximately 20 solidification strategies are available for producing building materials; these methods utilize various energy sources and additive materials and have diverse preparation conditions and durations. These approaches offer different construction capabilities, with some producing exceptionally high-strength materials, some exhibiting remarkable formation accuracy, and some boasting outstanding construction efficiency while requiring minimal equipment and energy.

The gap analysis report released by the International Space Exploration Coordination Group (ISECG) underscores the disruptive nature of the ISRU, emphasizing the need for an integrated design approach at the architectural level from the outset [8]. This disruption manifests in two key aspects: preparation and service. During the preparation stage, lunar construction faces unique challenges not encountered on Earth, where abundant energy, raw materials, machinery, and human laborers are readily accessible. On the Moon, engineering materials must be prepared under limited conditions. Moreover, the lunar environment poses severe challenges. The extremely low temperature and lack of solar energy make construction impractical at night. The ultravacuum and low-gravity conditions further complicate automated operations. During the service stage, lunar structures experience loads distinct from those on Earth. The internal pressure and structural sealing characteristics are major challenges for inhabited buildings. The low-gravity environment fundamentally changes the objectives of lunar construction materials, making gravity loads a secondary concern. Consequently, Earth-based structural systems and material preparation methods relying on gravity-bearing systems and compressed materials are not fully applicable to lunar construction. In addition, the Moon's extreme temperature and radiation can impact the durability of engineering materials. Materials utilized for lunar construction must be low-cost and high-performance. To achieve a low cost, resource consumption, energy requirements, and mechanical operations should be minimized during preparation. Conversely, to yield a high performance, materials must maintain exceptional mechanical properties in extreme lunar environments.

To investigate and assess solidification techniques, define the material requirements for lunar construction, and identify technical gaps and developmental pathways, scholars have conducted evaluations of these strategies. Table 1 [9–12] presents an overview of the evaluated techniques, highlighting the well-evaluated approaches identified in those works. However, the existing evaluations lack comprehensive summaries and accurate differentiation of various methods. To comprehensively assess a strategy, a researcher should evaluate all available technical solutions. In terms of accuracy, various techniques should be precisely defined and analyzed. For instance, high-temperature melting techniques should be more finely categorized into laser melting and solar melting methods given their substantial differences in energy utilization efficiency.

Table 2 [9–12] provides an organized list of evaluation indicators utilized by researchers, classified based on the goals of providing low-cost and high-performance materials. Indicators such as transportation and preparation costs fall under the low-cost category. The *in situ* ratio is used as a key indicator in all the evaluations. The preparation cost encompasses requirements such as energy, equipment, temperature, and time. For the high-performance category, compressive strength is often employed for assessment, along with environmental adaptability. Once the indicator system is established, subjective ratings of individual indicators are typically performed, followed by the consolidation of these indicators according to assigned weights. However, a primary challenge with this approach lies in the absence of a foundation for rating, primarily due to the lack of clearly defined construction goals and achievements.

In addition to qualitative evaluation, ongoing research has focused on quantitative evaluation. Metzger and Autry [12] conducted a quantitative study on construction techniques for lunar landing platforms by converting evaluation indicators into costs; for instance, they converted construction time into program delay costs and construction materials and equipment into transportation costs. The total cost of each technology can be calculated by applying this method, with microwave sintering being identified as the most economical option. This method is similar to the equivalent system mass (ESM) method proposed by National Aeronautics and Space Administration (NASA) [13], which converts technical shortcomings into the increased launch mass required to solve the problems. Converting different indicators into cost or mass is the focus of this method, requiring a precise description of the construction task and accurate estimates of cost or mass.

The primary contribution of this research includes a comprehensive review, precise classification, and quantitative evaluation of lunar regolith solidification and formation techniques. A database of technical parameters is established herein. Strategies are categorized based on the particle binding mechanism, followed by a detailed analysis of specific methods within each type. Subsequently, a quantitative evaluation method is proposed to objectively reflect the research status and identify gaps. This work provides an enhanced framework for classifying and evaluating lunar *in situ* material processing technologies, enabling well-informed decision-making for future lunar construction activities.

2. Classification of lunar regolith solidification and formation techniques

To address the issues of specificity and comprehensiveness, existing lunar regolith solidification and formation techniques are classified in this section. Solidification methods emphasize

Table 1
Evaluations of *in situ* material processing technique

Ref.	Evaluated technique[a]				Well-evaluated technique
	Reaction solidification	Sintering/melting	Bonding solidification	Confinement formation	
[9]	Wet mixing, dry mixed autoclaving	High-temperature sintering method	No method	No method	Dry mixed autoclaving method (improvement needed)
[10]	No method	Sintering, casting, Mg/Al SHS[b]	Sulfur binding, protein binding	Bagging	Dependent on demand
[11]	Extraterrestrial concrete	Melting and casting, sintering	Sulfur-bound regolith, regolith biocomposites	Sand-bagging	Regolith biocomposites
[12]	No method	Microwave sintering, pavers baked in an oven, solar sintering	High-temperature polymer infusion	Fabric matting	Microwave sintering (quantification)

[a] In the original text, the methods were not classified.
[b] Mg/Al SHS represents self-propagating high-temperature synthesis (SHS) based on magnesium (Mg) or aluminum (Al).

Table 2
Evaluated indicators of *in situ* material processing techniques.

Ref.	Transportation cost	Preparation cost	Application performance
[9]	Utilization ratio of lunar regolith	Raw material complexity, equipment complexity, energy demand, temperature, efficiency, technology maturity	Material strength
[10]	Binder mass	Processing energy	Compressive strength
[11]	Primary disadvantages (low *in situ* ratio)	Processing energy, primary disadvantages (low technological readiness)	Compressive strength, primary disadvantages (poor environmental adaptability)
[12]	Mass from Earth, number of rovers	Time to complete, energy expended, maximum power	No indicators

the bonding and cohesion between particles, which creates solid and unified materials, such as lunar regolith concrete and solidified regolith blocks. This process provides strength, stability, and structural integrity to the material. In contrast, formation methods focuses on shaping or molding a solid material into a desired form or structure. For lunar regolith, formation strategies involve confining the regolith within fabric bags or employing other methods to shape it into components or structures while maintaining its discrete solid state. In general, from the perspective of technical mechanisms, these technologies can be categorized into four groups: reaction solidification (RS), sintering/melting (SM), bonding solidification (BS), and confinement formation (CF) methods. Each category encompasses multiple specific technologies, as illustrated in Fig. 1.

2.1. Reaction solidification

RS techniques involve chemical reactions that are utilized to produce cementitious materials for the solidification of regolith and manufacturing of lunar concrete. Particles are bonded together through reacted compounds. RS strategies can be further classified based on different reaction principles, such as hydration reactions (often involving Portland cement and aluminate cement), Sorel cement reactions, geopolymer reactions, and hydrothermal synthesis reactions (also known as dry-mix/steam-injection (DMSI)). Fig. 2 [14–16] shows three examples of RS specimens.

- Raw materials for the hydration reaction include cementitious materials, aggregates, and water. The active substances in cementitious materials react with water to form binding

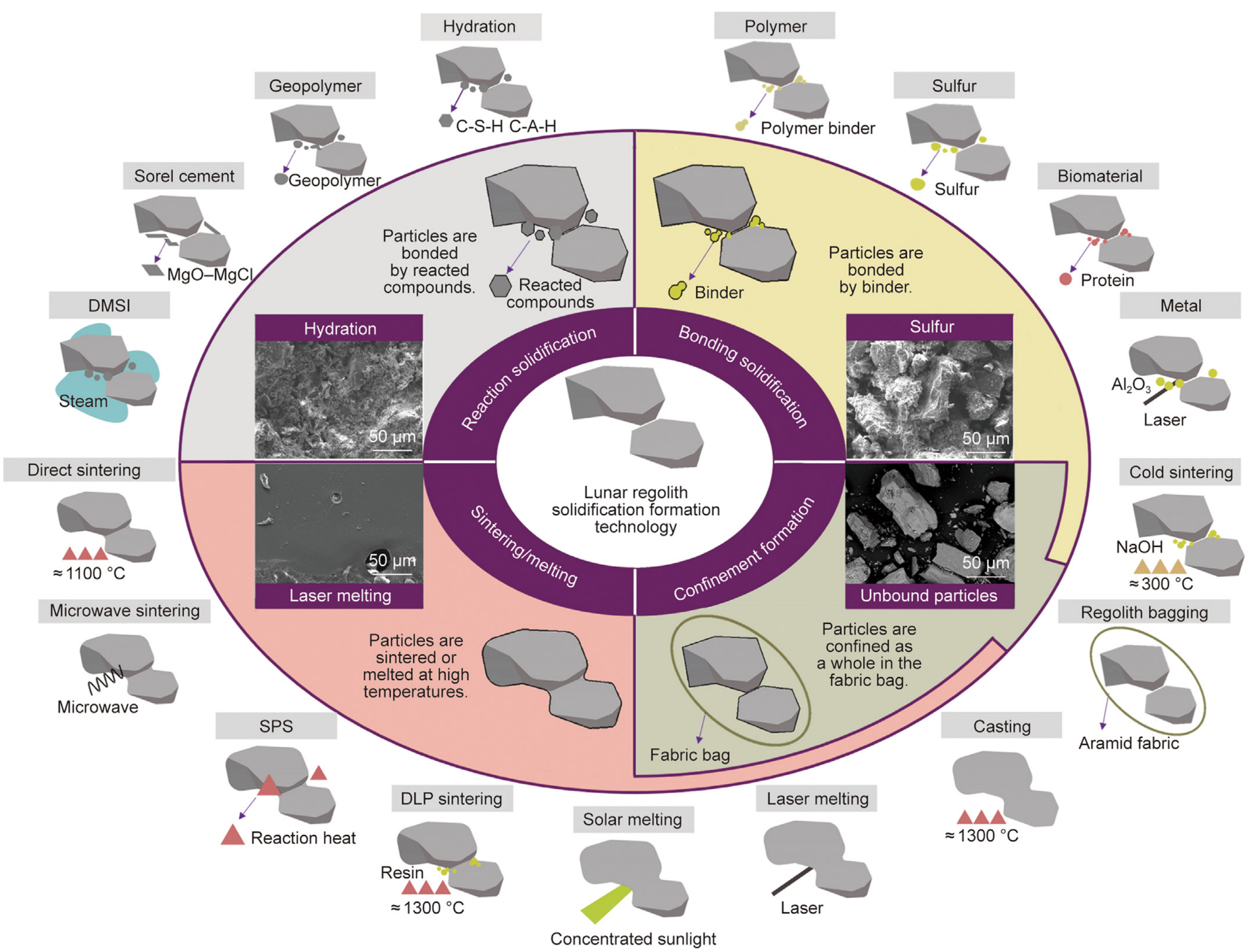

Fig. 1. Classification of existing lunar regolith solidification and formation strategies. C-S-H: hydrated calcium silicate; C-A-H: hydrated calcium aluminate; DMSI: dry-mix/steam-injection; SPS: self-propagating sintering; DLP: digital light processing.

hydration products, which bind aggregate particles together to form concrete. For example, the main hydration product of Portland cement is hydrated calcium silicate (C-S-H), while that of aluminate cement is hydrated calcium aluminate (C-A-H). Lin et al. [17] used a mixture of 54.1% real lunar regolith and aluminate cement to create lunar regolith concrete with a compressive strength of 75.6 MPa. Neves et al. [18] used Johnson Space Center-1A (JSC-1A) lunar regolith simulant, which comprises 75% of the mixture, and reacted it with Portland cement, achieving a compressive strength of 30 MPa.

- Sorel cement, also known as magnesium oxychloride cement, comprises the raw materials MgO and MgCl. The main reaction products are two $Mg(OH)_2$–MgCl–H_2O compounds. Cesaretti et al. [14] proposed the use of Sorel cement to solidify lunar regolith and developed a D-shaped additive manufacturing technique based on this reaction. These scholars used 85% of the "De NoArtri" (DNA-1) regolith simulant, and the samples achieved compressive strengths exceeding 20 MPa. The D-shaped technique had a much higher printing accuracy than that of other concrete three-dimensional (3D) printing techniques.
- The geopolymer reaction is based on the production of silicoaluminate compounds from silica–alumina-based raw materials in an alkaline environment, followed by coalescence to form a 3D reticulated polymer. Lunar regolith typically contains more than 60% silicoaluminate oxides, and geopolymer reactions require minimal water consumption, with 98% recyclable water [19]. Geopolymer reactions have received significant attention. In different experiments, the simulated lunar regolith mass fraction ranged from 74% to 94%, and the compressive strength of the solidified products varied from 9 to 80 MPa [15,20–29].
- The hydrothermal synthesis reaction DMSI utilizes Portland cement as a raw material. The reaction occurs in a saturated steam pressurized environment. The structure of the hydrate product varies with temperature and moisture content. This method can mitigate the effects of ultravacuum conditions on concrete curing. In the literature, the mass fraction of simulated lunar regolith in the DMSI method ranged from 70% to 90%, yielding solidified products with compressive strengths varying from 10 to 70 MPa [16,30–33].

2.2. Sintering/melting

SM solidification is a process that involves heating lunar regolith until it reaches a local or global melting state, facilitating solid-phase migration and bonding between regolith particles. The distinction between sintering and melting lies in the temperature conditions: sintering occurs below the material melting point, inducing vitrification in the material, while melting occurs above the melting point, causing the material to reach a flow state. Examples of sintering solidified instruments and specimens can be found in Fig. 3 [34–36].

According to different heating and pretreatment methods, sintering techniques can be divided into direct sintering, microwave sintering, and self-propagating sintering (SPS), which are heated by the following sources: electricity, microwaves, and chemical reactions, respectively.

- Direct sintering generates high temperatures through electric heating, typically at approximately 1100 °C [34,37–44]. In most direct heating studies, scholars did not use any admixtures, but a few researchers explored the use of binders, such as poly(lactic-*co*-glycolic acid) (PLGA) [41] or beeswax [42], for preforming (billeting). Directly heated samples exhibited high compressive strengths, exceeding 200 MPa in some cases [39,43]. In addition, Liu et al. [45] introduced photocurable resin for forming, which was subsequently solidified through sintering, achieving a relatively high compressive strength. Although the solidification mechanism is still sintering, this method can be classified as digital light processing (DLP) sintering due to the inclusion of additional formation methods.
- Microwave sintering heats lunar regolith with microwaves, achieving an *in situ* resource utilization rate of 100% [35,46–50]. The compressive strength of the microwave-sintered samples fluctuated widely, from a minimum of 12–13 MPa [46,47] to a maximum of 120 MPa [49]. These differences in strength were attributed to variations in the microwave absorption capabilities of the different simulated lunar regolith. Notably, while conducting microwave sintering experiments using real lunar regolith, Taylor and Meek [48] observed significant differences in the microwave absorption capabilities between real and simulated lunar regolith.
- SPS utilizes the heat released from chemical reactions. This technique involves exothermic reactions in which aluminum or magnesium are added to the lunar regolith, typically in contents of 10%–30%. The compressive strength achieved through SPS ranges from 10 to 18 MPa [36,51–54]. Corrias et al. [55] attempted to significantly increase the additive content by incorporating aluminum and iron oxide with a mass ratio reaching 90%, resulting in a compressive strength of 27 MPa.

Melting techniques include solar melting, laser melting, and casting. The first two methods bond particles in a point-by-point manner, while casting causes the lunar regolith to enter an overall flow state. Fig. 4 [56–58] shows examples of melting-solidified specimens.

- Solar melting uses optical equipment to concentrate sunlight to heat lunar regolith, achieving a 100% *in situ* material utilization ratio. Since there is no atmosphere on the Moon, sunlight can directly reach the lunar surface, providing an energy density over twice that on Earth [59]. This direct utilization of solar energy can minimize energy losses from conversion. However,

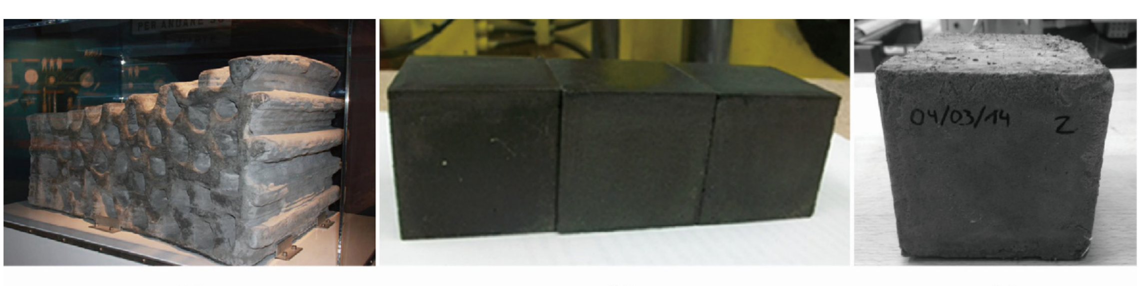

Fig. 2. Reaction solidified specimens: (a) Sorel cement reaction specimen [14]; (b) geopolymer reaction specimen [15]; and (c) DMSI specimen [16]. Reproduced from Refs. [14–16] with permission.

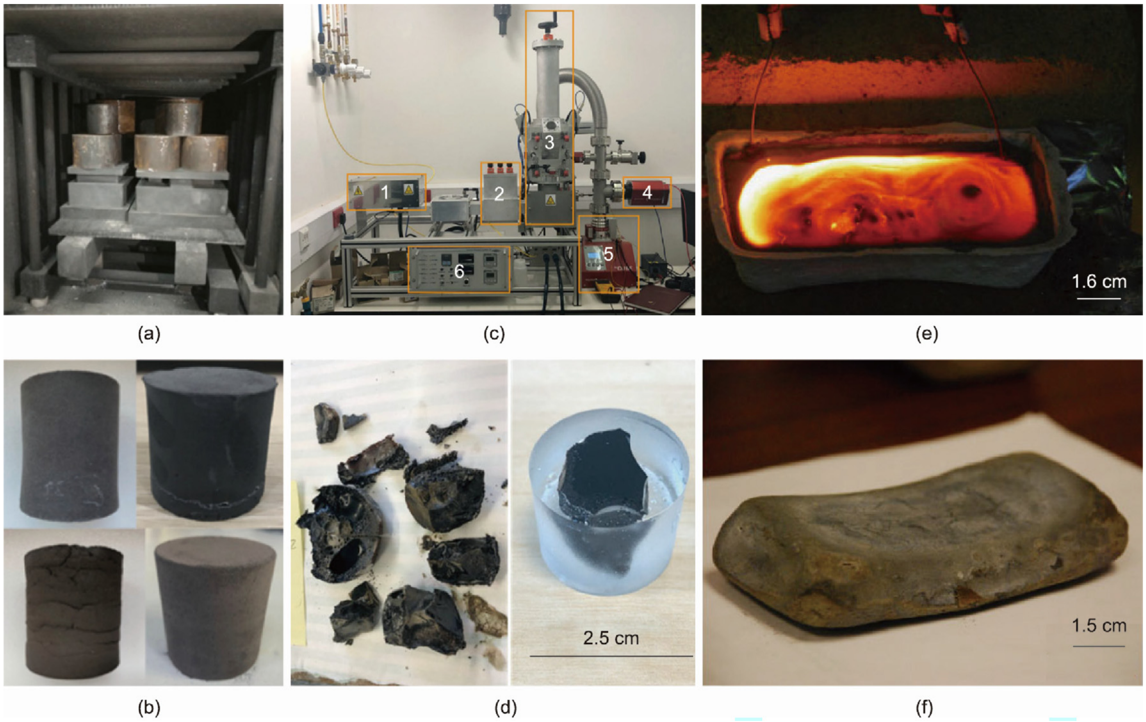

Fig. 3. Sintering solidified instruments and specimens: (a, b) direct sintering [34]; (c, d) microwave sintering [35]; and (e, f) self-propagating sintering [36]. Reproduced from Refs. [34–36] with permission.

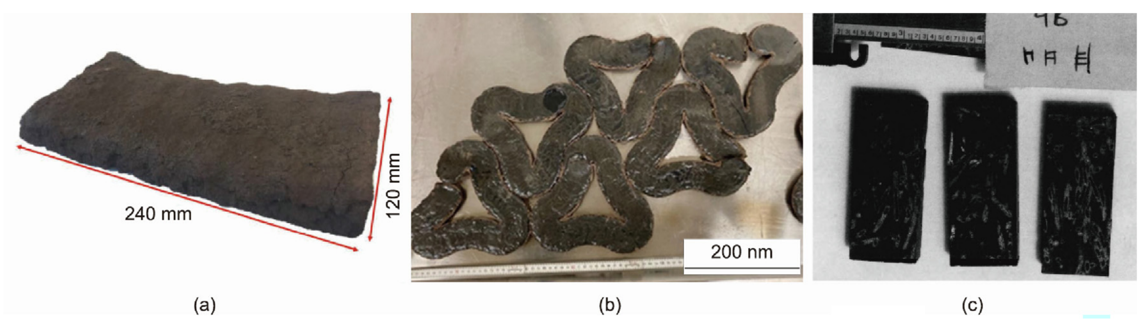

Fig. 4. Melting-solidified specimens: (a) solar melting [56]; (b) laser melting [57]; and (c) casting [58]. Reproduced from Refs. [56–58] with permission.

existing research on solar melting has shown relatively poor solidification results, with the compressive strengths of the resulting materials not exceeding 5 MPa [56,60–62].

- In laser melting, lunar regolith are heated with lasers, achieving an *in situ* material utilization ratio of 100%. In the United States and Germany, laser melting studies were conducted using JSC-1A simulated lunar regolith approximately ten years ago, but the resulting solidification strength was not reported [63,64]. Later, Goulas et al. [65] reported a solidification strength of 4.2 MPa, while Caprio et al. [66] experimentally achieved a strength of 31.4 MPa. The latest results came from Ginés-Palomares et al. [57], who used a high-power laser with a 100 mm-diameter laser spot to achieve high-strength and large-scale solidification with a compressive strength approaching 216 MPa.
- Casting completely heats lunar regolith to a molten state, and among all the tested techniques, this technique has the highest compressive strength [58,67,68]. Happel et al. [69] achieved a solidification strength of 538 MPa in their experiments.

2.3. Bonding solidification

BS involves using bonding materials to join regolith particles together. These bonding materials primarily include polymers, sulfurs, biomaterials, and metals. Examples of bonded solidified specimens are shown in Fig. 5 [11,70,71].

- Polymeric binders, including polyethylene [70], urethane [71], and silicone [66], are commonly used in lunar regolith solidification. The amount of binder added varies from 5% to 50%, and during the curing process, the binder is heated to its melting point (approximately 200 °C). Among the various polymeric binders tested, polyethylene has the highest curing strength. Lee et al. [72] combined 10% polyethylene with a basalt simulant and heated the mixture to 230 °C, obtaining a resulting material with a compressive strength exceeding 12 MPa.
- Sulfur is another extensively studied binder that is typically added at a concentration of 35% and cured at temperatures between 130 and 150 °C. The cured materials exhibit compressive strengths ranging from 7.8 to 33.8 MPa [70,73–75]. Omar

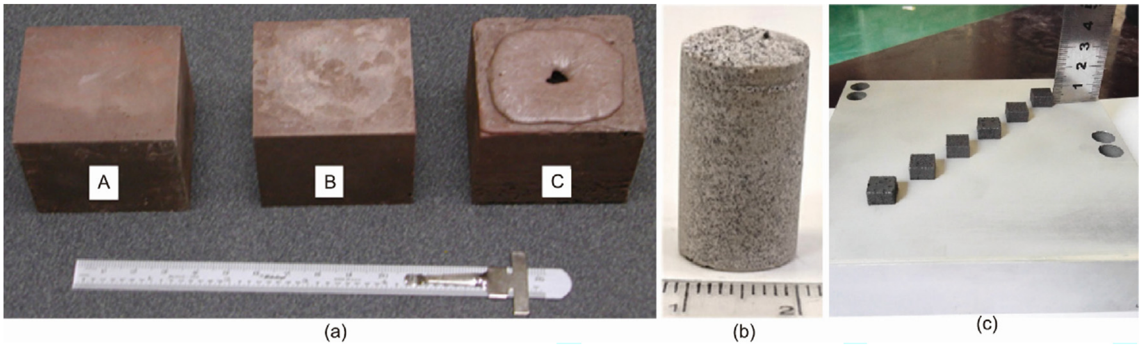

Fig. 5. Bonding solidified specimens: (a) sulfur bonding [70]; (b) biomaterial bonding [11]; and (c) metal bonding [71]. Reproduced from Refs. [11,70,71] with permission.

[74] enhanced the compressive strength to 45.5 MPa by adding 2% aluminum fibers to a mixture of sulfur and lunar simulants. However, sulfur binders are unsuitable for high-temperature environments, as sulfur sublimation occurs at temperatures above 95 °C. Therefore, sulfur bonding is feasible only in lunar polar regions or when appropriate thermal insulation measures are implemented.

- To maximize the utilization of resources transported to the lunar surface, biobased materials, such as urea and serum albumin, have been investigated as binders. Roedel et al. [10] mixed 22% serum albumin with JSC-1A lunar simulant, achieving a maximum compressive strength of 12.5 MPa. Roberts et al. [11] mixed 35% urea with lunar highlands simulant (LHS-1), resulting in a maximum compressive strength of 39.7 MPa.
- Liao et al. [71] proposed a method to prepare lunar regolith–AlSi10Mg composites. The lunar regolith simulant and AlSi10Mg powders were mixed at a weight ratio of 1:1 and solidified through selective laser melting (SLM) technique. In this method, the lunar regolith is melted and resolidified, forming a cohesive structure with molten aluminum acting as a binder. Although this approach combines aspects of both SM and BS from the perspective of particle bonding, it is classified as a BS method in this paper due to the binding role of aluminum. This approach effectively reduces brittleness and significantly improves the mechanical properties of the lunar regolith–AlSi10Mg composite, which has a compressive strength reaching 264 MPa, compared to that of the composite obtained by using laser melting alone.
- Additionally, Liu et al. [76] incorporated an NaOH solution and applied pressure during heating, achieving solidification at a low curing temperature. In this procedure, the NaOH solution dissolves the oxide clusters on the particle surface, generating a glass phase. The solidification mechanism relies on the glass phase connecting adjacent particles. Therefore, this process is classified as BS, although it is also known as cold sintering.

2.4. Confinement formation

CF, also known as regolith bagging, refers to the use of fabric bags to confine lunar regolith. Unlike bonding solidification, CF does not establish direct connections between particles but instead forms components through overall confinement; hence, it is classified as formation rather than solidification.

Smithers et al. [77] constructed lunar regolith bag structures using aramid fabrics (Kevlar) and nylon fabrics and conducted full-scale construction tests, as shown in Fig. 6 [77]. The compressive strength of the lunar regolith bag components ranged between 2 and 3 MPa. Additionally, Smithers et al. [77] evaluated the performance of various fabrics in service, including their tensile strength, high- and low-temperature resistance, bending resistance, radiation resistance, wear resistance, and hypervelocity impact. The scholars determined that polyarylester (Vectran) and aramid (Kevlar, Twaron) have potential applications. Finckenor [78] conducted aging tests on fabrics in a space environment and found that all the polymer fibers were eroded by atomic oxygen, which is the most significant environmental factor affecting fabrics. Therefore, protective coatings are required for radiation resistance. The maturity of regolith bagging is relatively high, and it has already been extensively used in terrestrial housing construction. For example, Nader Khalili constructed hundreds of superadobe structures using this strategy in Africa and South America [79]. In lunar construction projects, regolith bags have been utilized as primary structures [77,80], protective structures [81,82], and maintenance components [83].

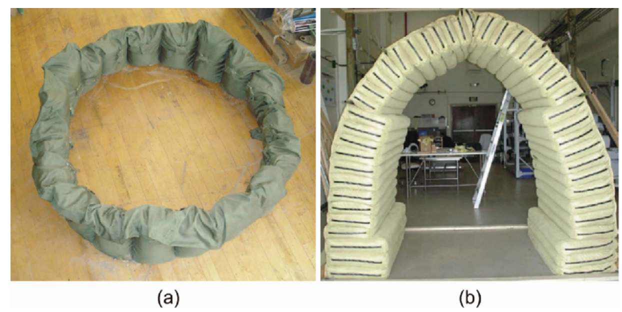

Fig. 6. Confinement formation specimens: (a) regolith bag berm and (b) regolith bag arch. Reproduced from Ref. [77] with permission.

3. Eight-indicator material evaluation method (8IMEM) and assessment results

3.1. Evaluation indicators and scoring criteria

The evaluation methodology employs a scoring system with eight indicators: *in situ* material ratio, curing temperature, curing time, implementation conditions, compressive strength, tensile strength, curing dimensions, and environmental adaptability. The first four indicators determine the technical requirements during material preparation, while the remaining four evaluate the mechanical properties of the material and its capability to withstand the harsh lunar environment. These indicators are fundamental for evaluating the overall performance and suitability of the aforementioned approaches for lunar construction. Each indicator is considered an independent variable and is rated on a scale from 1 to 5. A score of 5 indicates that a technique completely meets its construction needs and can be directly implemented, while a score of 1 suggests apparent technical flaws that may adversely affect the structure. A score of 3 reflects neutrality. The determination of the score threshold is based on construction requirements. The minimum requirement is considered the dividing line between positive and negative impacts (the neutral point). Then, combined with levels achieved in different studies, the requirement is extended on both sides to derive the thresholds for other scores. The detailed definitions and scoring thresholds are listed as follows:

- ***In situ* material ratio**: This indicator assesses the utilization (mass ratio) of *in situ* materials, primarily regolith. This ratio is a crucial factor regarding practical application on the Moon. Water is not considered an *in situ* material due to its limited availability and the challenges involved in its extraction, transportation, and utilization [8]. Equipment or reaction catalysts are ignored because they can be recycled. The main constraint for this indicator is the carrying capacity of a rocket. The Changzheng-9 (CZ-9) rocket, with a carrying capacity of 15–50 t when traveling to the Moon, is comparable to the American space launch system (SLS) [84]. The allocation of these loads to the landing system and other lunar missions leaves a limited share of building materials. Based on an estimate of 10 t, the carrying capacity of a single rocket indicates that the rocket can only transport approximately 2% of the total mass of a lunar structure (Table 3 [9,14,85]). Considering a neutral standard of 95%–98% *in situ* material utilization, which corresponds to completing the construction with one or two launch missions, a score of 5 is assigned to systems with 100% *in situ* resources, and a score of 1 is assigned to systems with 90% or less *in situ* resources, indicating a construction plan that requires more than five launch missions to complete.
- **Curing temperature:** This indicator evaluates the highest temperature required for heating. Besides SM techniques, it also encompasses the temperature conditions necessary for reactions (as in RS techniques) and the heating of binders (as in BS techniques). Specifically, solar melting and SPS sintering receive maximum scores because they utilize sunlight and reaction heat without additional energy requirements. This indicator is limited by equipment, energy consumption, and instantaneous power. Achieving uniform heating and efficient cooling becomes progressively challenging at high temperatures due to the lack of airflow in a vacuum environment, and precise measurement and control of high temperatures pose additional difficulties. Regarding energy consumption, a basic analysis shows that heating 1 t of regolith to 1000 °C requires at least 233 kW·h of energy (a specific heat capacity of 0.84 $kJ\cdot(kg\cdot K)^{-1}$ [86], excluding heat loss). This amount is equivalent to the power generation of a 100 m^2 photovoltaic array for six hours during a lunar day [87]. Considering equipment safety and energy consumption, 500 °C is established as a neutral score, and 1000 °C is set as 1 point. Temperatures less than or equal to 130 °C receive full marks, as this temperature is close to the temperature under direct sunlight on the lunar surface.
- **Curing time:** This indicator reflects the operating time required for curing, indirectly indicating energy consumption and efficiency. Specifically, the curing time of DMSI represents the time of steam curing, while hydration and geopolymer reactions require no curing equipment, earning them full marks in this indicator. For integral heating strategies, such as direct sintering, microwave sintering, casting, polymer bonding, and sulfur bonding, the heating processes define the curing time. The curing time for regolith bags refers to the time taken to fill and seal the bags. Unfortunately, the literature lacks data for additive manufacturing technologies, such as solar and laser melting. Point-by-point forming is significantly less efficient than activities such as sintering bricks, pouring concrete, or filling bags, resulting in relatively low scores for this indicator. Notably, curing time alone cannot be used to measure efficiency because curing times are not compared for the same volume, and further research is needed. The demand for this indicator mainly arises from considerations of energy consumption and the construction period. A basic analysis indicates that preparing 500 t of building materials in 24 lunar days (equivalent to 2 years) requires an average preparation rate of 60 kg of building materials per hour. Analogous to bricks on Earth, this speed requires a 100 L muffle furnace to burn a batch of bricks every four hours. Therefore, a neutral score is assigned to a curing time of 2–4 hours, a score of 5 is assigned to less than one hour, and a score of 1 is assigned to more than eight hours.
- **Implementation conditions:** This indicator evaluates the difficulty level in applying a technique, reflecting unquantifiable advantages and special needs. For example, microwave sintering has a high score due to the extreme coupling between the lunar regolith and microwave radiation. However, additional operations, such as screening and pressurization, result in a reduction in score. According to the definition of the five-level scale, a score of 3 suggests that the technique requires no special conditions, and most strategies fall into this level. A score of 2 indicates the presence of conditional requirements, with a focus on pressure and particle size limitations in this work. A score of 4 indicates natural advantages under lunar conditions. No technique receives 1 or 5 points.
- **Compressive strength** and **tensile strength:** These indicators assess the mechanical properties of a material. The compressive stress of a lunar structure is significantly reduced due to low gravitational load, while the tensile stress is relatively high in pressurized structures, approaching 1 MPa [9,88]. Temperature stresses can reach significant magnitudes. Construction solutions often involve the use of regolith coverings for insulation [89–91]. This approach transforms the issue into a systemic challenge rather than a mere material concern, allowing us to overlook the temperature stress. A neutral score is assigned to a tensile strength of 1–3 MPa, and a score of 5 is assigned to 10 MPa. Furthermore, a neutral score is assigned to a compressive strength of 5–15 MPa, which represents approximately 1/6

Table 3
Estimation of the total mass of a lunar structure.

Ref.	Scheme name and proposer	Design dimensions	Main building material	Density ($kg\cdot m^{-3}$)	Estimated total mass (t)	Proportion of CZ-9 carrying capacity (estimated as 10 t)
[9]	Xuanwu lunar habitation (HUST)	14.0 m in length, 8.0 m in width, 5.5 m in height	Regolith bricks	2500	500–700	1.4%–2.0%
[85]	SinterHub (NASA)	34 m^2 per person, 4 m in height	Sintered regolith	Not mentioned	400–600 (estimated for 3 people)	1.7%–2.5%
[14]	Lunar Outpost (ESA)	10 m in diameter, 5 m in height, 2 m in wall thickness	3D-printed concrete	900 (porous structure)	420	2.4%

HUST: Huazhong University of Science and Technology; ESA: the European Space Agency.

of the strength of blocks and concrete on Earth. A score of 5 is assigned to a compressive strength of 30 MPa. Methods lacking mechanical property data receive the lowest score of 1.

- **Curing dimensions:** This indicator refers to the maximum reported size of components in the literature. The construction volume of a lunar structure is large, and the ability to manufacture large components can simplify the construction process. Notably, the maximum reported size may not reflect the upper limit of the technology, as this size may be chosen for testing purposes. More accurate dimensional capabilities need to be collected. As a reference, the neutral score is assigned to dimensions of 25–50 mm, which meet the thickness requirements of standard masonry bricks. A score of 5 is assigned to dimensions at or above 150 mm, which correspond to the full-size requirements of standard bricks. Similarly, technologies lacking dimension data receive the minimum score of 1.
- **Environmental adaptability:** This qualitative indicator encompasses unquantifiable environmental impacts. For example, geopolymer components have been experimentally verified to exhibit good temperature resistance, while sulfur-bonded components are significantly affected by high temperatures. According to the definition of the five-level scale, a score of 3 indicates that no advantages or disadvantages have been reported. A score of 4 indicates adaptability to a certain environmental factor, and a score of 5 indicates verified adaptability to a simulated lunar environment. This definition corresponds to the concepts of laboratory environment and relevant environment in the Technology Readiness Level (TRL) [92]. A process that performs poorly in an extreme environment is given a score of 2. No technology is given a score of 1.

The evaluation indicators and their scoring criteria are presented in Table 4. Each indicator is assigned a weight to account for varying degrees of importance. These weights are subjective and can be adjusted based on construction conditions, adapting to different construction goals and stages of a project. The weight assigned to the *in situ* material ratio initially has a high value of 0.3 due to considerable transportation costs and difficulties, but it can be adjusted to a lower value as transportation costs decrease. Geotechnical materials are generally characterized as having strong compressive strengths and weak tensile strengths, suggesting that most regolith-based solidified materials cannot meet tensile requirements [9,93]. Therefore, the tensile strength is considered an important parameter for pressurized structures, and the compressive strength is not significantly important due to the low-gravity environment and conservative architectural design.

3.2. Evaluation of existing regolith solidification and forming technologies using 8IMEM

Data from published reports are used for evaluation in this study. Fig. 7 [10,11,14–18,20–34,36–50,52–58,60–77,94] presents the statistical findings of *in situ* material ratios and compressive strengths based on the assessed papers. In general, the *in situ* material ratios of SM and CF exceed 98%, except for those of SPS. Most RS and BS technologies range between 65% and 95%, which is relatively low for lunar construction. RS typically meets the benchmark for a compressive strength of 15 MPa, while SM and BS rely on the specific heating method and binder selection. However, CF does not meet compressive strength standards to date. Notably, the highest recorded compressive strength reaches 538 MPa. This remarkable achievement can be accomplished through casting technology, with a 100% *in situ* material ratio. The second-highest compressive strength recorded is 428.1 MPa, which can be attained by incorporating 30% photocurable resin for formation and sintering.

Compressive strength is one of the most extensively explored indicators in lunar regolith research, and it provides a valuable metric for assessing the quality of solidification. Three key factors that may affect the compressive strength are analyzed: the *in situ* material ratio, curing temperature, and curing time (Fig. 8). The compressive strength and *in situ* material ratio both demonstrate strong associations with the specific technical categories, as depicted in Fig. 8(a). The plot of compressive strength vs *in situ* material ratio reveals five different ranges, each corresponding to a particular category. Fig. 8(b) illustrates the correlation between the compressive strength and curing temperature. The curing temperatures are concentrated within two distinct ranges. SM predominantly operates at temperatures higher than 1050 °C, whereas other strategies operate at temperatures less than 250 °C. SM exhibits a relatively broad range of compressive strengths and can achieve high strengths. Regarding curing time, as shown in Fig. 8(c), SM, BS, and CF typically have curing times of less than 4 h, while RS usually requires a longer curing time exceeding 4 h.

Table 4
Eight evaluation indicators and scoring rules.

Category	Indicator	Unit	Weight	Scoring criteria				
				5	4	3	2	1
Technical requirement	*In situ* material ratio (%)	—	0.30	100	98–100	95–98	90–95	≤ 90
	Curing temperature	°C	0.10	≤ 130	130–200	200–500	500–1000	≥ 1000
	Curing time	h	0.10	≤ 1	1–2	2–4	4–8	≥ 8
	Implementation conditions	—	0.05	Especially suitable for lunar conditions	Suitable for lunar conditions	No special conditions required	Strict conditions required	Extremely strict conditions required
Application performance	Compressive strength	MPa	0.10	≥ 30	15–30	5–15	0–5	No data
	Tensile strength	MPa	0.15	≥ 10	3–10	1–3	0–1	No data
	Curing dimensions	mm	0.10	≥ 150	50–150	25–50	0–25	No data
	Environmental adaptability	—	0.10	Relevant environment validation	Laboratory environment validation	No advantages or disadvantages reported	Reduced performance	Significantly reduced performance

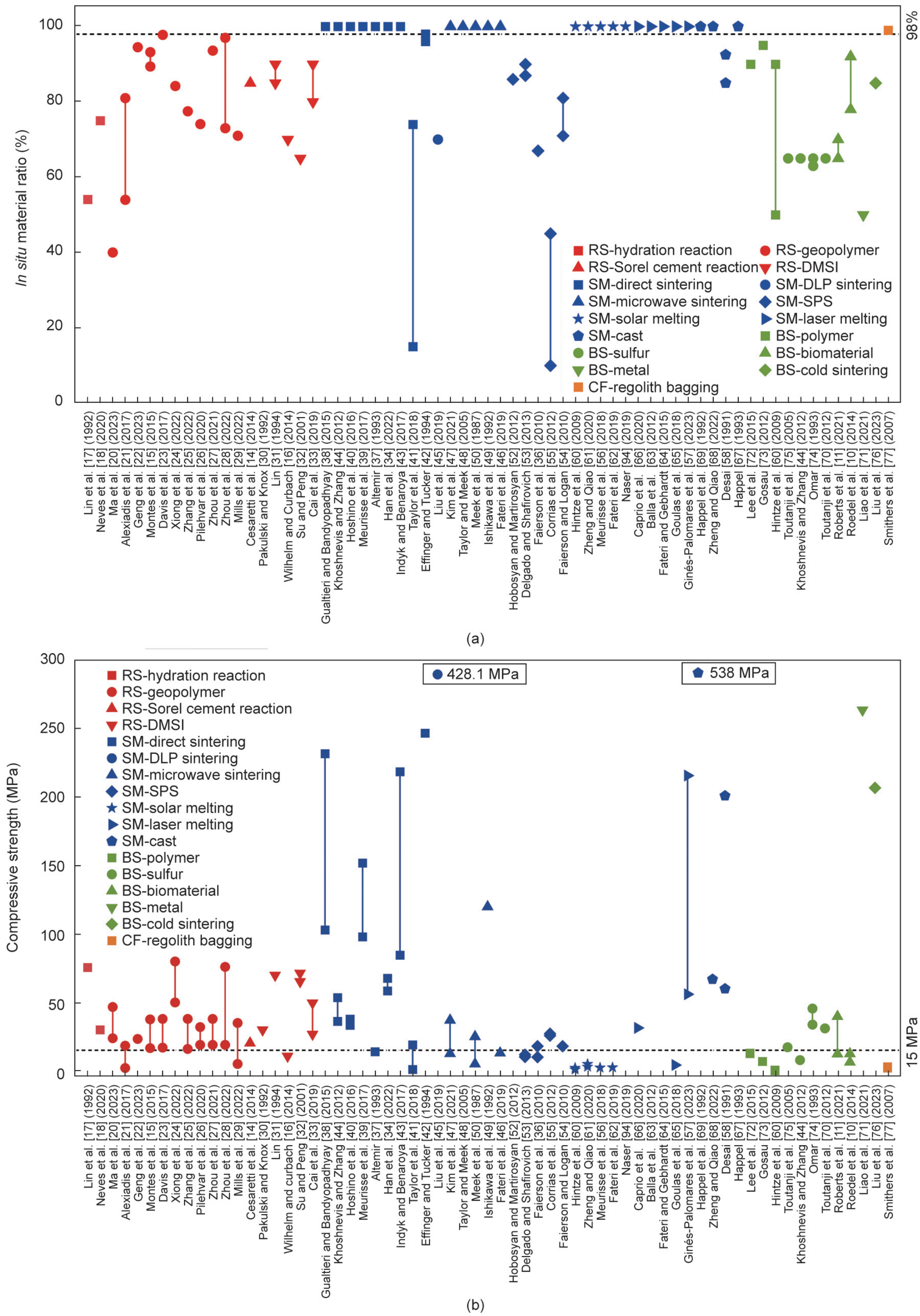

Fig. 7. (a) *In situ* material ratio and (b) compressive strength values in all evaluated reports.

Table 5 [10,11,14–18,20–34,36–50,52–58,60–77,94] provides comprehensive data from published reports, and Fig. 9 shows the weighted scores for various technologies. According to the evaluations, regolith bagging is the highest-rated technical solution, followed by casting, solar melting, direct sintering, and microwave sintering in that order, mainly due to its high *in situ* material ratio. The total score of the regolith bagging is 3.80, and the full score is achieved for curing temperature, time, and

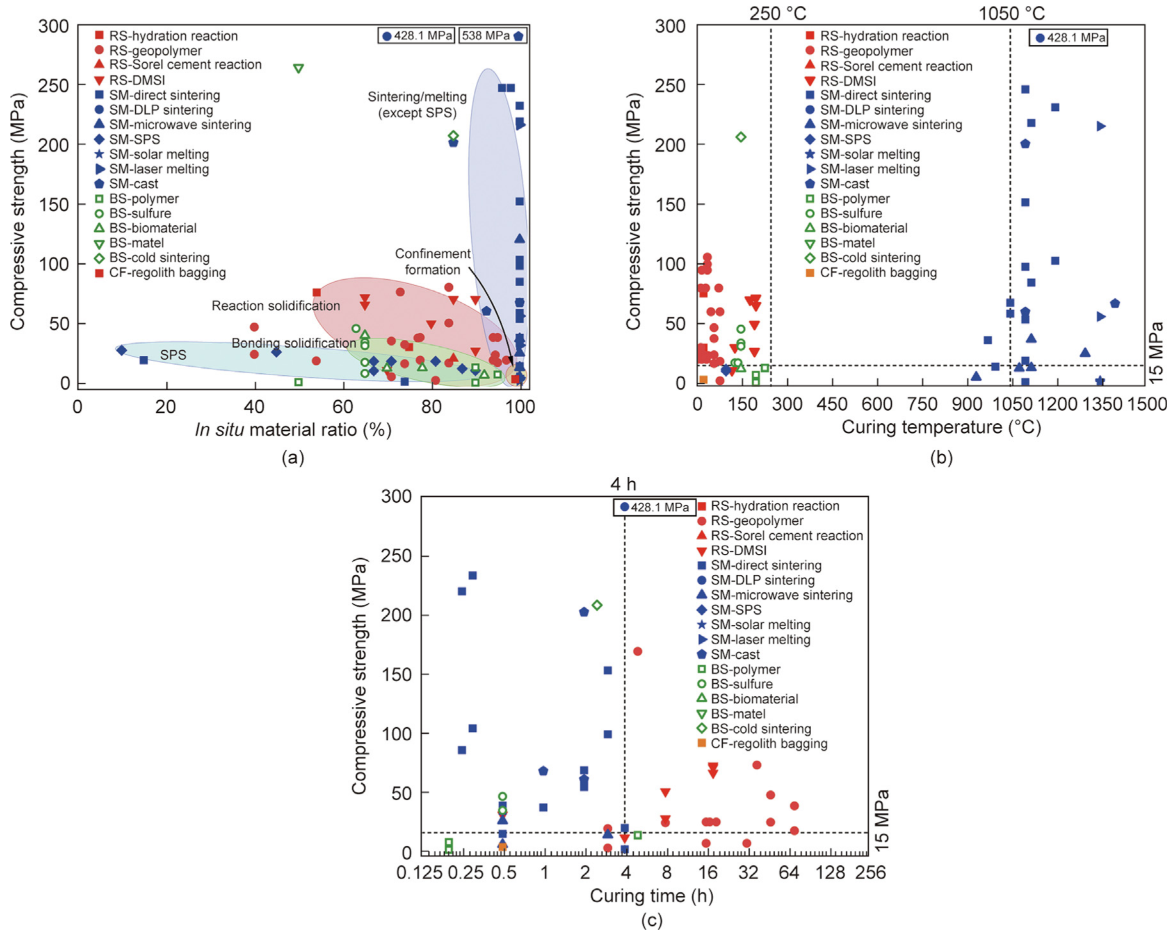

Fig. 8. Factors that affect the compressive strength. (a) *In situ* material ratio. The *in situ* material ratios of SM and CF are generally greater than 98%, except for SPS, while RS and BS have values generally between 65%–95%, which is relatively low for lunar structures. (b) Curing temperature. The curing temperature is divided into two groups. SM curing temperatures are generally higher than 1050 °C, while other curing temperatures do not exceed 250 °C. Notably, although SPS belongs to SM, it is considered a low-temperature strategy due to the lack of external heating and energy consumption. (c) Curing time. SM, BS, and CF have curing times that are usually less than 4 h, while RS has a curing time that is typically more than 4 h.

dimensions. The *in situ* material ratio is 99%, and the tensile strength is 2 MPa. Although the compressive strength falls slightly below the neutral score, it still reaches 2–3 MPa. Regolith bagging has no obvious shortcomings within the present evaluation system. SM strategies occupy the top positions in the ranking, mainly due to their 100% *in situ* material ratio and excellent performance in terms of other individual indicators. Casting has an extremely high strength, and solar melting involves the direct use of solar energy without performing additional energy conversion processes.

A sensitivity analysis is conducted to assess the impacts of the subjective indicator weights, focusing on two key indicators: the *in situ* material ratio and tensile strength. When adjusting the weight of a specific indicator, other weights are proportionally modified to keep the sum of the weights equal to 1. The analysis results indicate that a 20% change in the weights of the two analyzed indicators is feasible without significantly affecting the rankings. The top-ranking solution remains unchanged, but the subsequent rankings may experience minor changes within adjacent positions. This finding suggests that the weighted values exhibit sufficient stability.

Statistical measures, including the mean score, variance, and location square deviation (LSD), are calculated for gap analysis. The LSD value reflects the impact of a specific indicator on the final rankings by measuring the similarity between the single indicator ranking and the overall ranking. A lower LSD indicates a more significant impact on the ranking. Based on the analysis summarized in Table 6, several conclusions can be drawn:

(1) The tensile strength has the lowest mean score, demonstrating the shortcomings of the recent state of research, namely, the lack of reported tensile strength and typically low tensile strength in cured samples.

(2) Environmental adaptability requires further research. The mean environmental adaptability score is moderate, and the variance is extremely low. Most related studies have not involved investigations of the impact of the lunar environment.

(3) Strategies that performed better in terms of curing temperature, compressive strength, and curing dimensions tend to be ranked lower, probably because they often require the addition of other materials, which reduces the *in situ* material ratio. Each technical solution has advantages and disadvantages and needs to be weighed according to the construction requirements.

4. Lunar habitat construction scheme based on the regolith bagging method

4.1. Overall lunar construction plan

Lunar exploration projects are massive national undertakings, and the planning of these projects by major countries and

Table 5
Evaluation and scoring of existing *in situ* material processing strategies.

Source	Technology	*In situ* material ratio (%)	Curing temperature (°C)	Curing time (h)	Implementation conditions			Compressive strength (MPa)	Tensile strength (MPa)	Curing dimensions (mm)	Environmental adaptability
					Curing pressure (MPa)	Selected particle size (μm)	Unique adaptability				
[17]	Hydration reaction	54.1	—	—	—	—	—	75.635	8.315	25 × 25 × 25	Maintenance required
[18]		75	—	—	—	—	—	30	—	150 × 150 × 150	Maintenance required
[20]	Geopolymer	40	60	48	—	—	—	23.8–46.7	—	—	Extreme temperature tested
[11]		54–81	80	3	—	—	—	2–18.4	13	10 × 10 × 10	—
[22]		94.5	40	8	0.06	—	—	23.3	7.98	40 × 10 × 10	—
[15]		77–84	60	72	0–14	—	—	16.6–37.6	—	ϕ20 × 25	—
[23]		94.3	26–106	24–168	0–14	—	—	17–38	—	—	—
[24]		84.2	60	168	—	—	—	50–80	—	20 × 20 × 20	—
[25]		77.5	30–100	24–72	—	—	—	16–38	5.7	160 × 40 × 40	—
[26]		74.1	80	6	—	—	—	16–32	—	30 × 30 × 30	Low temperature tested
[27]		93.6	95	24–72	—	—	—	19–38	—	—	Vacuum tested
[28]		73–97	20–80	168	—	—	—	19–76	6.3	—	—
[29]		71	20	168	—	—	—	5–35	—	15 × 15 × 15	High temperature tested
[14]	Sorel reaction	85	—	—	—	—	—	20.35	—	395 × 395 × 195	—
[30]	DMSI	100	130	0.5	0.2	—	—	30	—	—	Special reaction environment required
[31]		85–90	180	18	—	—	—	70	—	—	
[16]		70	120	4	0.2	—	—	10.7	—	100 × 100 × 100	
[32]		65	200	18	—	—	—	65.3–71.5	—	100 × 100 × 100	
[33]		90	98	24	25	—	—	26.8–49.6	—	—	
[38]	Direct sintering	100	1200	0.3	145	25–212	—	103–232	—	ϕ7 × 12.7	—
[44]		100	975–1100	1–2	—	—	—	36.2–53.5	—	50.8 × 16.8 × 7.6	—
[40]		100	—	0.5	—	—	—	33.3–37.8	7.2–8.2	210 × 100 × 60	Vacuum sintering tested
[39]		100	1100	3	255	—	—	98–152	—	ϕ20	Vacuum sintering tested
[37]		100	1000	0.5	253	—	—	14	—	—	—
[34]		100	1050	2	0.025	—	—	58.45–67.68	—	ϕ50	Vacuum sintering tested
[43]		100	1120	0.25	4	0–212	—	84.6–218.8	—	ϕ12 × 19	—
[41]		15–74	1100	4	—	—	—	1–19	—	—	—
[42]		96–98	1100	24	276–414	0–180	—	247	—	—	—
[45]	DLP sintering	70	1150	4	—	—	—	428.1	129.5	—	Extreme temperature tested
[47]	Microwave sintering	100	1080–1120	—	—	0–850	Extreme coupling of lunar regolith to microwave radiation	12.6–37	—	—	Extreme temperature tested
[48]		100	—	—	—	—		—	—	—	—
[50]		100	936–1300	0.5	—	—		5–25	—	—	—
[49]		100	—	—	—	—		120	—		—
[46]		100	1120	3	—	—		13	—	ϕ20 × 40	—
[52]	SPS	86	—	—	—	—	—	—	—	ϕ13 × 30	—
[53]		87–90	100	—	—	—	—	10.2–11.8	—	ϕ25 × 33	—
[36]		67	—	—	—	—	—	10–18	—	ϕ25 × 50	—
[55]		10–45	—	—	—	—	—	25.8–27.2	—	ϕ11 × 25	—
[54]		71–81	—	—	—	—	—	18	—	ϕ25 × 90	—
[60]	Solar melting	100	1350	—	—	—	Higher energy density of sunlight compared to Earth	0.90–2.14	—	2.5–6	Lunar dust abrasion tested
[61]		100	—	—	—	—		2.94–4.95	—	5 × 5	—
[56]		100	—	—	—	—		2.31	—	240 × 130 × 50	—
[62]		100	—	—	—	—		2.49	0.23–0.55	20 × 20 × 70	Vacuum sintering tested
[94]		100	—	—	—	—		—	—	—	Lunar dust abrasion tested but performed poorly
[66]	Laser melting	100	—	—	—	—	—	31.4	—	60 × 60 × 20	—
[63]		100	—	—	—	50–150	—	—	—	ϕ10 × 25–ϕ10 × 30	—
[64]		100	—	—	—	0–63	—	—	—	10 × 10 × 3	—

Table 5 (*continued*)

Source	Technology	*In situ* material ratio (%)	Curing temperature (°C)	Curing time (h)	Implementation conditions: Curing pressure (MPa)	Selected particle size (μm)	Unique adaptability	Compressive strength (MPa)	Tensile strength (MPa)	Curing dimensions (mm)	Environmental adaptability
[65]	Casting	100	–	–	–	0–125	–	4.2	–	5 × 5 × 5	–
[57]		100	1350	–	–	–	–	56–216	–	200 × 200 × 15	–
[69]		100	–		–	–	–	538	34.5	–	–
[68]		100	1400	1	–	–	–	67	100.7	2 × 10 × 10	–
[58]		85–92.5	1100	2	–	–	–	60.0–201.2	4.1–29.5	25 × 2.5 × 6.25	–
[67]		100	–		–	–	–	–	–		–
[72]	Polymer bonding	90	230	5	–	–	–	12.6–12.9	–	50 × 50 × 50	–
[73]		95	200	0.2	–	–	–	6.9	–		–
[60]		50–90	200	0.2	–	–	–	0.14–0.55	–	ϕ60 × 5	The vacuum environment affects polymer film formation
[75]	Sulfur bonding	65	130–140	–	–	–	–	17.2	–	50 × 50 × 50	Sublimation problems in vacuum and high-temperature environments
[44]		65	–	–	–	–	–	7.8	–		
[74]		63–65	150	0.5	–	–	–	33.8–45.5	–	50 × 50 × 50	
[70]		65	150	–	–	–	–	31	–	50 × 50 × 50	
[11]	Biomaterial bonding	65–70	–	–	–	–	–	12.3–39.7	–	ϕ10	–
[10]		78–92	–	–	0.085	–	–	6.3–12.5	–	152 × 152 × 25	–
[71]	Metal bonding	50	–	–	–	0–75	–	264	–		–
[76]	Cold sintering	85	150	2.5	200	0–75	–	207	–	ϕ15 × 12	Extreme temperature tested
[77]	Regolith bagging	99	–	0.5	–	–	–	2–3	2	500 × 500 × 200	–

organizations is crucial. The United States Artemis program is divided into two phases: targeting landing and construction. Phase 2 aims to establish a sustainable human presence in the cislunar space and on the lunar surface [1]. As part of this phase, NASA plans to build the Gateway, a space station around the Moon, including living modules of the Habitation and Logistics Outpost (HALO) and the International Habitation (I-HAB). For surface construction, NASA has envisioned the surface habitat (SH), which is a metallic and inflatable hybrid structure that can house a two-person crew for surface stays reaching 30 days [95]. In addition, NASA plans to enhance the ability of SH, allowing it to support a four-person crew for 60 days over its 15-year design life [96]. Another construction plan, the foundation surface habitat (FSH), features a rigid lower part and an inflatable upper part. The FSH is designed to accommodate a four-person crew for activities lasting 30–60 days [97].

In 2016, the European Space Agency (ESA) proposed the Moon Village program, which advocates a permanent surface outpost that should be executed as an international collaborative effort. Moon Village is an international community initiative that serves as a springboard and testing ground for crewed flights into deep space [98]. The One Moon construction plan, developed by Skidmore Owings & Merrill (SOM) in collaboration with the ESA and Massachusetts Institute of Technology (MIT), features a structure comprising a rigid structural frame and an inflatable structural shell. A 500 mm-thick sintered regolith protective shell is used to shield the structure from radiation [99].

China's manned lunar exploration project consists of two stages: landing and residence. During the residence phase, China plans to establish a mobile laboratory and a research station for long-term presence on the Moon. According to the preliminary concept, the lunar mobile laboratory is a pressurized lunar rover that can move over a wide range and support the short-term stay of astronauts. Moreover, ISRU techniques can be used to construct surface facilities and expand them to scientific research stations. In addition, China proposed the ILRS, a large-scale long-term research platform for short-term manned experiments and long-term autonomous operations involving international cooperation [2,3].

Based on the lunar construction conditions and the long-term goals of the ILRS, we divide the overall construction process into four stages: the laboratory stage, research station stage, residence stage, and habitat stage. Each stage has specific functions and construction goals, as outlined in Table 7.

- **Laboratory stage:** supporting scientific research projects not requiring habitation. Construction tasks include site selection, ground levelling and hardening, and protective wall construction to shield research equipment from sunlight and lunar dust.
- **Research station stage:** supporting astronauts temporarily scientific research. The living spaces for astronauts gradually transition from landers to lunar buildings. Construction tasks include equipment foundations and working units. Moreover, the site and protective walls are expanded according to the scale of lunar exploration activities.
- **Residence stage:** meeting all the work and life requirements of astronauts on the Moon. The functional positioning of the residential unit is similar to that of a space station. Lunar base capabilities are further enhanced, and areas are connected by roads for high-speed transportation. Construction tasks include roads, takeoff and landing platforms, and the functional module expansions.
- **Habitat stage:** serving as a self-sustaining habitat for human life and production on the Moon and as a relay station for deep space exploration. Construction tasks include living units and greenhouses to fulfill the living and production needs of lunar residents.

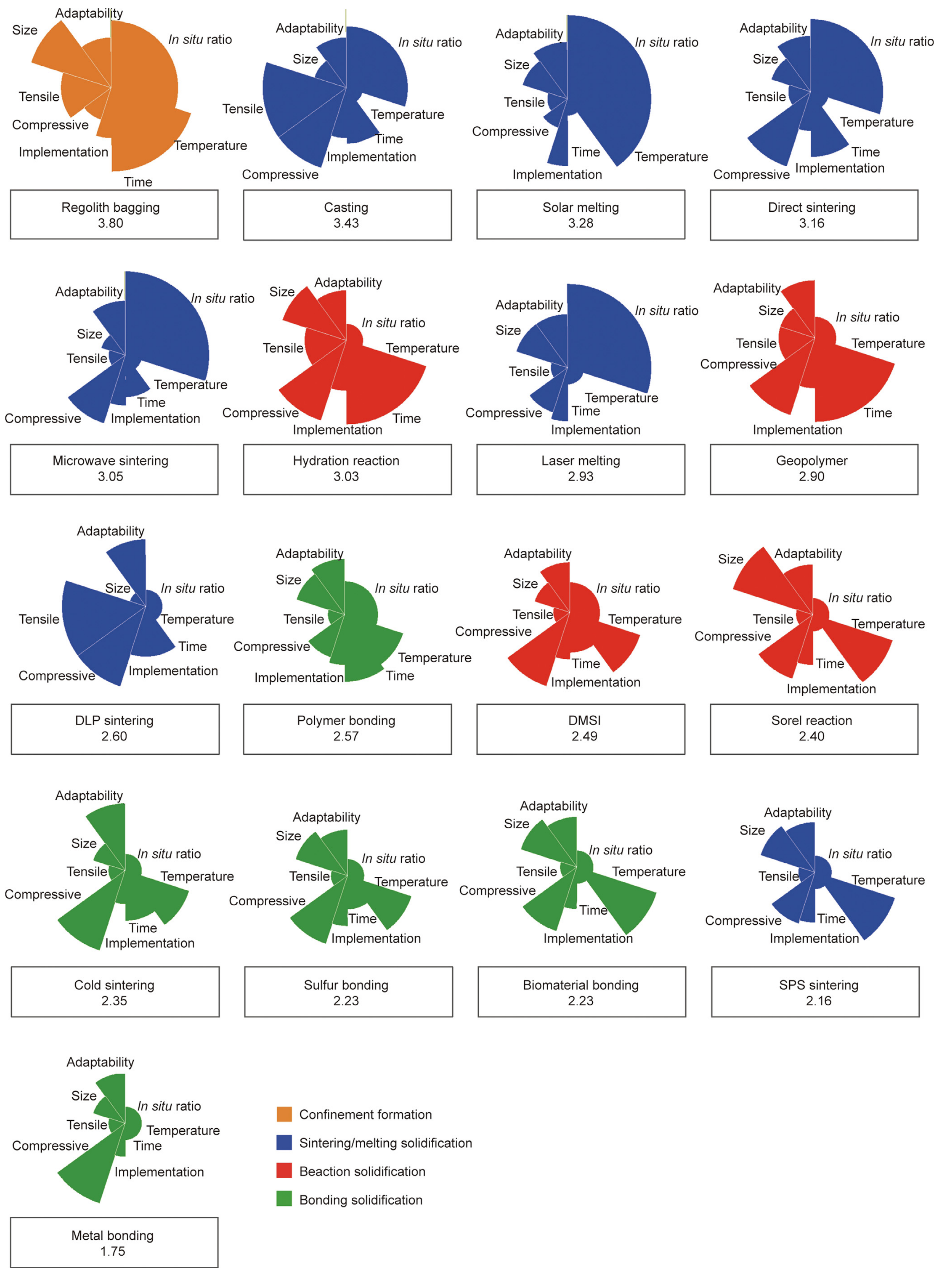

Fig. 9. Scores for lunar regolith solidification and formation strategies. The techniques are sorted by score. Regolith bagging is the highest-rated technical solution, followed by casting, solar melting, direct sintering, and microwave sintering.

Table 6
Statistical analysis of evaluation indicators.

Statistical measure	*In situ* material ratio	Curing temperature	Curing time	Implement conditions	Compressive strength	Tensile strength	Curing dimensions	Environmental adaptability
Mean score	2.36	3.36	2.65	2.87	4.00	1.78	2.85	3.22
Variance	2.68	3.16	2.20	0.21	1.14	1.74	1.18	0.11
LSD	10.94	49.32	21.65	23.06	54.18	13.53	50.38	33.94

Table 7
Overall plan for lunar construction.

Stage	Functional orientation	Construction goals		
		Site and road	Structure	Inhabited buildings
Laboratory	Mainly scientific research projects not requiring habitation	Site leveling and hardening	Protective wall	No task at this stage
Research station	Short-term research involving astronauts	Site hardening, equipment foundation	Protective wall	Working units
Residence	Meeting the work and living needs of astronauts	Roads, takeoff and landing platforms, equipment foundations	Protective wall	Working units, living units
Habitat	Fully autonomous operation	Roads, equipment foundations	Protective wall	Working units, living units, greenhouse

4.2. Lunar habitat solution based on regolith bag structures

A lunar habitat is designed to establish an ILRS and prepare for future expansion. The habitat is strategically located at the South Pole due to its heightened scientific research value and relatively mild environment. To fulfill the requirements of long-term residence, experimentation, and surface exploration, the habitat is composed of three main construction targets: sites, protection structures, and inhabited buildings. Fig. 10 shows the versatility of regolith bags with customizable geometries and matching processes for different construction purposes.

Site treatment for lunar habitats can be categorized into two types according to the treatment objective: hardening and solidification. Hardening is used to meet load-bearing requirements, such as constructing spacecraft takeoff and landing platforms, roads, and structural foundations. Solidification aims to prevent wear or conductive damage caused by lunar dust. Solidified components do not require high strength but do require a high volume. Elongated regolith bags are sequentially filled and laid on the site for dust prevention and for providing some load-bearing capacity.

The primary function of the protection structure is to act as a barrier against harsh lunar elements, such as dust and direct sunlight. This structure is primarily designed to withstand gravitational and temperature loading. The construction volume is substantial, necessitating cost-effective, convenient, and low-maintenance techniques. Protection structures are constructed by arranging regolith bags in a stacked formation, similar to river embankments on Earth.

Inhabited buildings are the most complex and important construction targets. These buildings must ensure internal environmental safety by maintaining suitable pressure, temperature and humidity conditions, in addition to resistance to radiation and micrometeorites. For long-term missions, inhabited buildings should offer sufficient interior space and functional zoning. A modular design is adopted to facilitate expansion. Each module is calculated based on the minimum space requirements for short-term tasks [100], providing a usable area of 15 m^2 or a pressurized volume of 40 m^3. An airbag is utilized for airtightness and temporary support. Regolith bags and airbags are pre-connected on Earth, with the inner airbag inflated first, followed by filling the regolith bags. The interconnected regolith bags form an arch shape, enabling resistance to the extreme lunar environment. The arch structure can continue to function even in the case of airbag pressure loss, providing dual protection for inhabited buildings. A preliminary calculation of transportation demand indicates that the external material mass of a single bag is approximately 0.4 kg (dimensions of 600 mm $\times$ 300 mm $\times$ 150 mm). To build an inhabited building unit, approximately 0.7 t of external materials is needed, including 0.5 t of bags, 0.2 t of inflatable airbags, and compressed

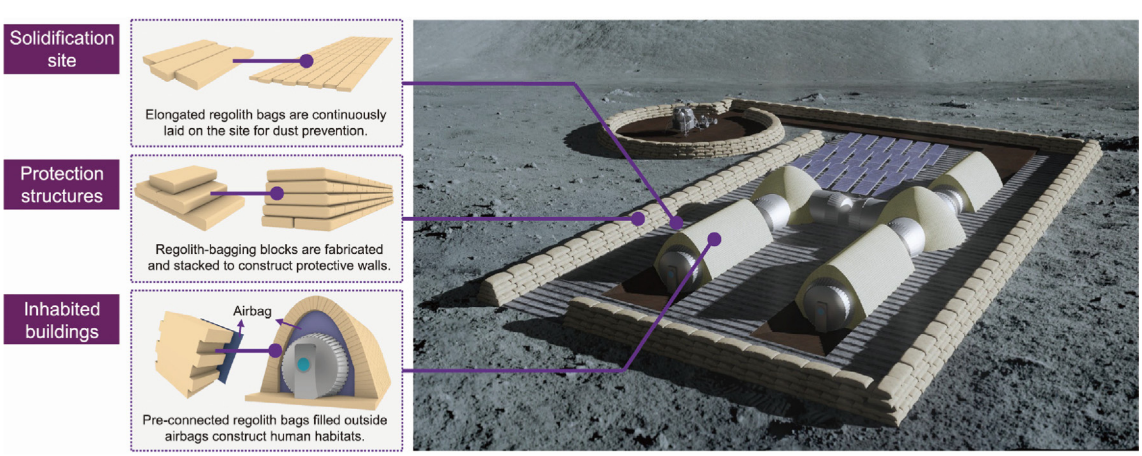

Fig. 10. Lunar habitat solution based on regolith bag structures.

air. Construction equipment primarily consists of robotic arms equipped with various end effectors to perform excavation, filling, and sealing functions. The weight and power of the equipment need further evaluation.

5. Discussion

5.1. Evaluation system

An evaluation system comprises scoring rules and indicators. Scoring rules can be categorized as qualitative or quantitative, with the latter generally being more objective. In quantitative methods, it is crucial to determine reasonable score thresholds and weights. The score threshold is established by comparing construction requirements with actual capabilities, identifying areas where capabilities fall short, and measuring the extent of the shortcoming. Various methods are employed to represent this shortcoming in different forms. The ESM method converts shortcomings into equivalent masses [101], the total cost method transforms them into incremental costs [12], and the 8IMEM translates them into scores below the neutral score. In addition, the five-level scale allows for quantifying the advantages, measuring and assigning points to areas where capabilities meet or exceed needs. This approach is similar to calculating the transportation mass saved by a technical feature in the ESM method. 8IMEM is convenient and allows for the autonomous scoring of new research, facilitating regular updates of the technical database.

In this article, the weight is subjectively determined. Several evaluation approaches employ the analytical hierarchy process (AHP) to compute weights [102], essentially involving a subjective comparison of the importance of two indicators, with the subjective impact mitigated through multiple comparisons. Further research is needed for theoretical exploration and continuous refinement of score thresholds and weights to achieve a more objective evaluation and adapt to the evolving technical landscape.

This article classifies indicators for lunar construction materials into low-cost and high-performance categories; this strategy is commonly used in other studies [9–12]. Among the specific indicators, the *in situ* ratio and compressive strength are widely recognized. The preparation cost exhibits some dispersion, with the complexity, energy, temperature, time, and/or efficiency being frequently considered as parameters. While high compressive strength is often associated with high performance in existing evaluations, this criterion is not exhaustive. To enhance the assessment, we introduce additional indicators, such as tensile strength, dimensions, and environmental adaptability.

The factors of economy and energy consumption are indirectly reflected in the evaluation. The economy or cost is considered a technical goal rather than a standalone indicator, encompassing every indicator of technical application. In this study, the cost is subdivided into transportation and preparation costs, which are measured through indicators such as the *in situ* ratio and implementation conditions. The lack of precise data on energy consumption poses a significant challenge to this evaluation. For instance, the estimated energy for microwave sintering varies significantly, spanning from 24 to 200 $kJ \cdot g^{-1}$. Similar uncertainties exist for direct sintering and solar melting [103]. Herein, we address energy consumption to some extent through indicators such as curing temperature and time, but more accurate measurements require further research.

5.2. Evaluation results

SM solidification strategies are scored highly in this study, as they typically achieve a 100% *in situ* material ratio and demonstrate outstanding performance in terms of individual indicators. Among SM techniques, casting stands out because it yields the highest compressive and tensile strengths, making it particularly suitable for scenarios with extremely demanding mechanical performance requirements. However, this method requires the highest heating temperature among the approaches and a relatively long processing time; thus, its broad application may be constrained by an inadequate energy supply. Solar melting involves the direct utilization of solar energy as the heating source, providing a significant advantage in terms of energy supply. If this technology can overcome the challenges related to solidification strength and size, it can become a crucial technique for lunar construction. China's Lunar and Deep Space Exploration [104] states that one of the scientific payloads of Chang'e-8 is "to utilize solar energy to *in situ* melt lunar regolith and fabricate functional components, to measure their mechanical and thermal properties, and able to be assembled by robots." This indicates that the advantage of SM techniques has been recognized by China in the near-term lunar exploration efforts, which aligns with the evaluation results in this paper. RS and BS receive lower ratings due to their low *in situ* material ratios, emphasizing the urgent need to produce reaction materials and binders *in situ*.

ISRU and transportation are intricately linked in complementary and mutually reinforcing relationships. ISRU products can influence transportation and the development of other surface elements/capabilities, while ISRU systems rely on resources and capabilities from other surface elements/capabilities [8]. In the early stages of lunar construction, 100% *in situ* material construction is unnecessary because it may cause increasingly complex material handling issues. As large-scale construction and maintenance activities commence, advancements in *in situ* production technologies are expected. This progress can gradually replace Earth-transported materials with *in situ* materials, allowing for the introduction of additional construction technologies on the Moon.

5.3. Advantages of regolith bagging

Regolith bagging offers advantages over other methods. This procedure achieves acceptable application performance with considerably low technical requirements, scoring the highest in the 8IMEM evaluation. One key advantage is the low requirements for filling raw materials. Since the regolith particles used in bags are not required to participate in chemical reactions or phase changes, particles of different components and sizes can be used. The *in situ* material ratio can reach 99%. Furthermore, regolith bag structures require minimal energy and equipment inputs due to the absence of heating and curing processes. Only fabric bags, which constitute 1% of the total mass, need to be transported from Earth, and they can be efficiently compressed to fit the launch volume. The fabric provides adequate tensile strength for the components. Although the compressive strength does not reach neutrality, it still meets most construction needs in low-gravity environments. Regarding application performance, regolith bagging enables the quick manufacturing of large-scale components and thus large-scale structures.

Regolith bagging is versatile, as the shapes and dimensions of regolith bags can vary to form different structural and nonstructural components. Different regolith bag combinations allow the formed structures to adapt to various scenarios, especially for large-scale construction. At the component and structural levels, a lunar habitat solution based on regolith bag structures has been developed, including the construction method and structural composition from site to building. Regolith bag structures can achieve site solidification and protective wall construction while matching existing rocket launch capabilities. In the future, with the assistance of high-thrust rockets, regolith bagging technology may facilitate the construction of inhabited buildings and lunar habitats.

6. Conclusions

In this study, a comprehensive review, precise classification, and quantitative evaluation of lunar regolith solidification and formation strategies are provided. An evaluation method called 8IMEM is developed considering eight indicators. Among the evaluated techniques, regolith bagging is a promising approach for lunar construction. A construction scheme for the lunar habitat is proposed, outlining the overall construction plan, developmental stages, and specific construction requirements from the site to the buildings. Finally, a lunar habitat solution based on regolith bag structures is devised. The following key findings are drawn from this study:

- Regolith solidification and formation technologies can be classified into four main groups based on their technical mechanisms: RS, SM, BS, and CF. Among them, RS, SM, and BS enable the bonding of regolith particles using reacted compounds, melting and solidifying of materials, and binders, respectively, while CF features fabric for overall confinement.
- The 8IMEM method is developed as an evaluation system utilizing eight indicators to quantitatively evaluate the effectiveness and feasibility of these technologies for lunar implementation. Among these methods, regolith bagging technology has the highest rating due to its high *in situ* material ratio, relatively low technological requirements, and absence of significant shortcomings, making it the preferred choice for large-scale construction in the future. The casting technique can produce regolith-based materials with the highest strength, but the high energy requirement and demanding manufacturing conditions limit its application in large-scale construction. Solar melting is promising and has universal applicability for extraterrestrial construction due to the highest *in situ* material ratio and the low energy requirement, but further development is needed in terms of mechanical strength and component size.
- The proposed habitat construction scheme consists of four stages—laboratory, research station, residence, and habitat. This scheme eventually evolves into a comprehensive building cluster with hardened sites, roads, protective structures, and inhabited buildings. The regolith bag structure is a highly feasible design with widespread adoption potential in lunar construction. The key advantages of this process lie in large formation components with various shapes, fast construction speeds, reliable tensile strengths, and low demands for construction materials, equipment, and energy.

In this paper, future research directions in the field of lunar construction are highlighted. At the material level, it is crucial to investigate the performance and feasibility of these methods in extreme lunar environments. All of these techniques should be adaptively improved, such as by incorporating coatings to increase the resistance of regolith bag materials to extreme temperature, radiation, and abrasion conditions. At the system design level, lunar construction demands a collaborative approach that integrates perspectives from construction, materials, structures, and techniques. In-depth evaluations of architectural plans, structural forms, and construction strategies are essential for identifying viable solutions and research directions for the future.

Acknowledgments

This work was supported by the National Natural Science Foundation of China (42241109), the Guoqiang Institute, Tsinghua University (2021GQG1001), and the New Cornerstone Science Foundation through the XPLORER PRIZE.

Compliance with ethics guidelines

Charun Bao, Daobo Zhang, Qinyu Wang, Yifei Cui, and Peng Feng declare that they have no conflicts of interest or financial conflicts to disclose.

References

[1] Smith M, Craig D, Herrmann N, Mahoney E, Krezel J, McIntyre N, et al. The artemis program: an overview of NASA's activities to return humans to the moon. In: Proceedings of the 2020 IEEE Aerospace Conference; 2020 Mar 7–14; Big Sky, MT, USA. New York City: IEEE; 2020. p. 1–10.
[2] Song J. China emphasizes international cooperation in future lunar and deep space exploration. Bull Chin Acad Sci 2019;2:72–9.
[3] Jones A, Patel P, Waltz E, Bajema N. The latest developments in technology, engineering, and science: news. IEEE Spectr 2021;58:6–13.
[4] Flahaut J, van der Bogert CH, Crawford IA, Vincent-Bonnieu S. Scientific perspectives on Lunar exploration in Europe. npj Microgravity 2023;9:50.
[5] Sasaki H, Director J. JAXA's Lunar exploration activities. In: Proceedings of the 62nd Session of the Committee on the Peaceful Uses of Outer Space (COPUOS); 2019 Jun 12–21; Vienna, Austria. Vienna: United Nations Office for Outer Space Affairs; 2019. p. 12–21.
[6] An HJ. South Korea's space program. Asia Policy 2020;15:34–42.
[7] Hoshino T, Wakabayashi S, Ohtake M, Karouji Y, Hayashi T, Morimoto H, et al. Lunar polar exploration mission for water prospection—JAXA's current status of joint study with ISRO. Acta Astronaut 2020;176:52–8.
[8] International Space Exploration Coordination Group. *In-situ* resource gap assessment report. Vienna: International Space Exploration Coordination Group; 2021 Apr 21.
[9] Zhou C, Chen R, Xu J, Ding L, Luo H, Fan J, et al. *In-situ* construction method for lunar habitation: Chinese super mason. Autom Construct 2019;104:66–79.
[10] Roedel H, Lepech M, Loftus D. Protein—regolith composites for space construction. Earth Space 2014;2014:291–300.
[11] Roberts AD, Whittall DR, Breitling R, Takano E, Blaker JJ, Hay S, et al. Blood, sweat, and tears: extraterrestrial regolith biocomposites with *in vivo* binders. Mater Today Bio 2021;12:100136.
[12] Metzger PT, Autry GW. The cost of Lunar landing pads with a trade study of construction methods. New Space 2023;11:94–123.
[13] Levri J, Fisher JW, Jones HW, Drysdale AE, Ewert MK, Hanford AJ et al. Advanced life support equivalent system mass guidelines document. Washington, DC: National Aeronautics and Space Administration; 2003.
[14] Cesaretti G, Dini E, De Kestelier X, Colla V, Pambaguian L. Building components for an outpost on the lunar soil by means of a novel 3D printing technology. Acta Astronaut 2014;93:430–50.
[15] Montes C, Broussard K, Gongre M, Simicevic N, Mejia J, Tham J, et al. Evaluation of lunar regolith geopolymer binder as a radioactive shielding material for space exploration applications. Adv Space Res 2015;56:1212–21.
[16] Wilhelm S, Curbach M. Manufacturing of lunar concrete by steam. Earth Space 2015;2014:274–82.
[17] Lin T, Love H, Stark D. Physical properties of concrete made with Apollo 16 lunar soil sample. In: Proceedings of the Second Conference on Lunar Bases and Space Activities of the 21st Century; 1988 Apr 5–7; Huston, TX, USA. Washington, DC: NASA Conference Publication; 1992.
[18] Neves JM, Ramanathan S, Suraneni P, Grugel R, Radlińska A. Characterization, mechanical properties, and microstructural development of lunar regolith simulant–portland cement blended mixtures. Constr Build Mater 2020;258:120315.
[19] Wang KT, Lemougna PN, Tang Q, Li W, Cui XM. Lunar regolith can allow the synthesis of cement materials with near-zero water consumption. Gondwana Res 2017;44:1–6.
[20] Ma S, Jiang Y, Fu S, He P, Sun C, Duan X, et al. 3D-printed Lunar regolith simulant-based geopolymer composites with bio-inspired sandwich architectures. J Adv Ceram 2023;12:510–25.
[21] Alexiadis A, Alberini F, Meyer ME. Geopolymers from lunar and Martian soil simulants. Adv Space Res 2017;59:490–5.
[22] Geng Z, Zhang L, Pan H, She W, Zhou C, Zhou H, et al. *In-situ* solidification of alkali-activated lunar regolith: Insights into the chemical and physical origins. J Clean Prod 2023;391:136147.
[23] Davis G, Montes C, Eklund S. Preparation of lunar regolith based geopolymer cement under heat and vacuum. Adv Space Res 2017;59:1872–85.
[24] Xiong G, Guo X, Yuan S, Xia M, Wang Z. The mechanical and structural properties of lunar regolith simulant based geopolymer under extreme temperature environment on the moon through experimental and simulation methods. Constr Build Mater 2022;325:126679.
[25] Zhang R, Zhou S, Li F. Preparation of geopolymer based on lunar regolith simulant at *in-situ* lunar temperature and its durability under lunar high and cryogenic temperature. Constr Build Mater 2022;318:126033.
[26] Pilehvar S, Arnhof M, Pamies R, Valentini L, Kjøniksen AL. Utilization of urea as an accessible superplasticizer on the moon for lunar geopolymer mixtures. J Clean Prod 2020;247:119177.

[27] Zhou S, Yang Z, Zhang R, Zhu X, Li F. Preparation and evaluation of geopolymer based on BH-2 lunar regolith simulant under lunar surface temperature and vacuum condition. Acta Astronaut 2021;189:90–8.
[28] Zhou S, Zhu X, Lu C, Li F. Synthesis and characterization of geopolymer from lunar regolith simulant based on natural volcanic scoria. Chin J Aeronauti 2022;35:144–59.
[29] Mills JN, Katzarova M, Wagner NJ. Comparison of lunar and Martian regolith simulant-based geopolymer cements formed by alkali-activation for *in-situ* resource utilization. Adv Space Res 2022;69:761–77.
[30] Pakulski DM, Knox KJ. Steam injection system for lunar concrete. In: Engineering, Construction, and Operations in space-III: Space'92 Proceedings of the 3rd International Conference; 1992 May 31–Jun 4; Denver, CO, USA. Online: The SAO/NASA Astrophysics Data System; 1992. p. 1347–58.
[31] Lin T. Dry-mix/steam-injection method for producing high-strength concrete in one day. Spec Publ 1994;149:665–78.
[32] Su N, Peng YN. The characteristics and engineering properties of dry-mix/steam-injection concrete. Cement Concr Res 2001;31:609–19.
[33] Cai L, Ding L, Luo H, Yi X. Preparation of autoclave concrete from basaltic lunar regolith simulant: effect of mixture and manufacture process. Constr Build Mater 2019;207:373–86.
[34] Han W, Ding L, Cai L, Zhu J, Luo H, Tang T. Sintering of HUST-1 lunar regolith simulant. Constr Build Mater 2022;324:126655.
[35] Lim S, Bowen J, Degli-Alessandrini G, Anand M, Cowley A, Levin PV. Investigating the microwave heating behaviour of lunar soil simulant JSC-1A at different input powers. Sci Rep 2021;11:2133.
[36] Faierson EJ, Logan KV, Stewart BK, Hunt MP. Demonstration of concept for fabrication of lunar physical assets utilizing lunar regolith simulant and a geothermite reaction. Acta Astronaut 2010;67:38–45.
[37] Altemir D. Cold press sintering of simulated lunar basalt. In: Proceedings of the 24th Lunar and Planetary Science Conference; 1993 Mar 15–19; Houston, TX, USA. Online: NASA Astrophysics Data System; 1993. p. 23–4.
[38] Gualtieri T, Bandyopadhyay A. Compressive deformation of porous lunar regolith. Mater Lett 2015;143:276–8.
[39] Meurisse A, Beltzung JC, Kolbe M, Cowley A, Sperl M. Influence of mineral composition on sintering Lunar regolith. J Aerosp Eng 2017; 30(4):040170.
[40] Hoshino T, Wakabayashi S, Yoshihara S, Hatanaka N. Key technology development for future Lunar utilization—block production using Lunar regolith. Trans Jpn Soc Aeronaut Space Sci Aero Technol Japan 2016;14: Pk_35–40.
[41] Taylor SL, Jakus AE, Koube KD, Ibeh AJ, Geisendorfer NR, Shah RN, et al. Sintering of micro-trusses created by extrusion-3D-printing of lunar regolith inks. Acta Astronaut 2018;143:1–8.
[42] Effinger M, Tucker D. Statistical design study of lunar ceramic. Washington, DC: National Aeronautics and Space Administration Marshall Space Flight Center; 1994.
[43] Indyk SJ, Benaroya H. A structural assessment of unrefined sintered lunar regolith simulant. Acta Astronaut 2017;140:517–36.
[44] Khoshnevis B, Zhang J. Extraterrestrial construction using contour crafting. In: Proceedings of the 2012 International Solid Freeform Fabrication Symposium: An Additive Manufacturing Conference; 2012 Aug 6–8; Austin, TX, USA. Austin: University of Texas at Austin; 2012.
[45] Liu M, Tang W, Duan W, Li S, Dou R, Wang G, et al. Digital light processing of lunar regolith structures with high mechanical properties. Ceram Int 2019;45:5829–36.
[46] Fateri M, Cowley A, Kolbe M, Garcia O, Sperl M, Cristoforetti S. Localized microwave thermal posttreatment of sintered samples of lunar simulant. J Aerosp Eng 2019;32:04019051.
[47] Kim YJ, Ryu BH, Jin H, Lee J, Shin HS. Microstructural, mechanical, and thermal properties of microwave-sintered KLS-1 lunar regolith simulant. Ceram Int 2021;47:26891–7.
[48] Taylor LA, Meek TT. Microwave sintering of lunar soil: properties, theory, and practice. J Aerosp Eng 2005;18:188–96.
[49] Ishikawa Y, Sasaki T, Higasayama T. Simple and efficient methods to produce construction materials for lunar and Mars bases. In: Engineering, Construction, and Operations in space-III: Space'92 Proceedings of the 3rd International Conference; 1992 May 31–Jun 4; Denver, CO, USA. Online: The SAO/NASA Astrophysics Data System; 1992. p. 1335–46.
[50] Meek T, Vaniman D, Blake R, Godbole M. Sintering of lunar soil simulants using 2.45 GHz microwave radiation. In: Abstracts of the Lunar and Planetary Science Conference; 1987 Mar 16–20; Houston, TX, USA. Washington, DC: NASA Lunar and Planetary Institute; 1987. p. 635.
[51] Ferguson RE, Shafirovich E, Mantovani JG. Combustion joining of regolith tiles for *in situ* fabrication of launch/landing pads on the moon and mars. In: Proceedings of the 16th Biennial International Conference on Engineering, Science, Construction, and Operations in Challenging Environments; 2018 Apr 9–12; Cleveland, OH, USA. Houston: Lunar and Planetary Institute; 2018. p. 281–8.
[52] Hobosyan M, Martirosyan K. Sintering of regolith by activated thermites: a novel approach for lunar *in-situ* resource utilization. In: Proceedings of the 43rd Annual Lunar and Planetary Science Conference; 2012 Mar 19–23; The Woodlands, TX, USA. Houston: Lunar and Planetary Institute; 2012. p. 1019.
[53] Delgado A, Shafirovich E. Towards better combustion of lunar regolith with magnesium. Combust Flame 2013;160:1876–82.
[54] Faierson EJ, Logan KV. Geothermite reactions for *in situ* resource utilization on the moon and beyond. In: Proceedings of the Earth and Space 2010: Engineering, Science, Construction, and Operations in Challenging Environments; 2010 Mar 14–17; Honolulu, HI, USA. Washington, DC: American Society of Civil Engineers; 2010. p. 1152–61.
[55] Corrias G, Licheri R, Orrù R, Cao G. Self-propagating high-temperature reactions for the fabrication of Lunar and Martian physical assets. Acta Astronaut 2012;70:69–76.
[56] Meurisse A, Makaya A, Willsch C, Sperl M. Solar 3D printing of lunar regolith. Acta Astronaut 2018;152:800–10.
[57] Ginés-Palomares JC, Fateri M, Kalhöfer E, Schubert T, Meyer L, Kolsch N, et al. Laser melting manufacturing of large elements of lunar regolith simulant for paving on the Moon. Sci Rep 2023;13(1):15593.
[58] Desai CS. Development and mechanical properties of structural materials from lunar simulant. Tucson: NASA Space Engineering Research Center for Utilization of Local Planetary Resources; 1991.
[59] Appelbaum J, Flood DJ. Solar radiation on Mars. Sol Energy 1990;45:353–63.
[60] Hintze P, Curran J, Back T. Lunar surface stabilization via sintering or the use of heat cured polymers. In: Proceedings of the 47th AIAA Aerospace Sciences Meeting including The New Horizons Forum and Aerospace Exposition; 2009 Jan 5–8; Orlando, FL, USA. Reston: American Institute of Aeronautics and Astronautics; 2009.
[61] Zheng W, Qiao G. Mechanical behavior of the metal parts welded with extraterrestrial regolith simulant by the solar concentrator in ISRU & ISRF application. Adv Space Res 2020;65:2303–14.
[62] Fateri M, Meurisse A, Sperl M, Urbina D, Madakashira HK, Govindaraj S, et al. Solar sintering for Lunar additive manufacturing. J Aerosp Eng 2019;32 (6):04019101.
[63] Balla VK, Roberson LB, O'Connor GW, Trigwell S, Bose S, Bandyopadhyay A. First demonstration on direct laser fabrication of lunar regolith parts. Rapid Prototyping J 2012;18:451–7.
[64] Fateri M, Gebhardt A. Process parameters development of selective laser melting of Lunar regolith for on-site manufacturing applications. Int J Appl Ceram Technol 2015;12:46–52.
[65] Goulas A, Binner JGP, Engstrøm DS, Harris RA, Friel RJ. Mechanical behaviour of additively manufactured lunar regolith simulant components. Proc Inst Mech Eng Part L: J Mater Des Appl 2018;233:1629–44.
[66] Caprio L, Demir AG, Previtali B, Colosimo BM. Determining the feasible conditions for processing lunar regolith simulant via laser powder bed fusion. Addit Manuf 2020;32:101029.
[67] Happel JA. Indigenous materials for lunar construction. Appl Mech Rev 1993;46:313–25.
[68] Zheng W, Qiao G. Microstructure, thermophysical, and mechanical properties of bulk glass prepared from molten lunar regolith simulant. Adv Space Res 2022;69:3130–9.
[69] Happel JA, Willam K, Shing B. Prototype lunar base construction using indigenous materials. In: Engineering, Construction, and Operations in space-III: Space'92 Proceedings of the 3rd International Conference; 1992 May 31–Jun 4; Denver, CO, USA. Online: The SAO/NASA Astrophysics Data System; 1992. p. 112–22.
[70] Toutanji HA, Evans S, Grugel RN. Performance of lunar sulfur concrete in lunar environments. Constr Build Mater 2012;29:444–8.
[71] Liao H, Zhu J, Chang S, Xue G, Pang J, Zhu H. Lunar regolith–AlSi10Mg composite fabricated by selective laser melting. Vacuum 2021;187:110122.
[72] Lee TS, Lee J, Yong AK. Manufacture of polymeric concrete on the Moon. Acta Astronaut 2015;114:60–4.
[73] Gosau JM. Regolith stabilization and building materials for the lunar surface. In: Proceedings of the 13th ASCE Aerospacespace Division Conference on Engineering, Science, Construction, and Operations in Challenging Environments, and the 5th NASA/ASCE Workshop On Granular Materials in Space Exploration; 2012 Apr 15–18; Pasadena, CA, USA. Washington, DC: American Society of Civil Engineers; 2012. p. 243–9.
[74] Omar HA. Production of lunar concrete using molten sulfur. Report. Washington, DC: The National Aeronautics and Space Administration; 1993. NASA Grant NAG8-278.
[75] Toutanji H, Glenn-Loper B, Schrayshuen B. Strength and durability performance of waterless lunar concrete. In: Proceedings of the 43rd AIAA Aerospace Sciences Meeting and Exhibit; 2005 Jan 10–13; Reno, NV, USA. Reston: American Institute of Aeronautics and Astronautics; 2005.
[76] Liu Z, Li J, Yang C, Wang X, Xiao J, Wang L et al. Cold sintering of lunar regolith simulant: an energy-efficient and high-reliable strategy for building lunar bases. 2023. SSRN 4371120.
[77] Smithers GA, Nehls MK, Hovater MA, Evans SW, Miller JS, Broughton RM Jr, et al. A one-piece lunar regolith bag garage prototype. Report. Huntsville: NASA Marshall Space Flight Center; 2007. No. NASA/TM-2007-215073.
[78] Finckenor M. Comparison of high-performance fiber materials properties in simulated and actual space environments. Technical Memorandum. Huntsville: NASA Marshall Space Flight Center; 2017. No. NASA/TM-2017-219634.
[79] Zhao Z, Lu Q, Jiang X. An energy efficient building system using natural resources—superadobe system research. Procedia Eng 2015;121:1179–85.
[80] Ruess F, Zacny K, Braun B. Lunar *in-situ* resource utilization: regolith bags automated filling technology. In: Proceedings of the AIAA SPACE 2008 Conference & Exposition; 2008 Sep 9–11; San Diego, CA, USA. Reston: American Institute of Aeronautics and Astronautics; 2008.

[81] Mei H, Bao W, Yu D, Liu P, Wang Y, Pan W, et al. Research on building plans design for future lunar base. J Deep Space Explor 2022;9:553–9. Chinese.

[82] Tóth AR, Bagi K. Analysis of a lunar base structure using the discrete-element method. J Aerosp Eng 2011;24:397–401.

[83] Soleymani T, Trianni V, Bonani M, Mondada F, Dorigo M. Autonomous construction with compliant building material. In: Intelligent Autonomous Systems 13: Proceedings of the 13th International Conference IAS-13 (Advances in Intelligent Systems and Computing, 302); 2014 Jul 15–18; Padova, Italy. Berlin: Springer; 2016. p. 1371–88.

[84] Harvey B. China in space: the great leap forward. Berlin: Springer Nature; 2019.

[85] Rousek T, Eriksson K, Doule O. SinterHab. Acta Astronaut 2012;74:98–111.

[86] Robie RA, Hemingway BS, Wilson WH. Specific heats of lunar surface materials from 90 to 350 degrees Kelvin. Science 1970;167:749–50.

[87] Colozza AJ. Small lunar base camp and *in situ* resource utilization oxygen production facility power system comparison. Report. Cleveland: Glenn Research Center; 2020. NASA/CR-2020-220368.

[88] Zhou C, Tang B, Ding L, Sekula P, Zhou Y, Zhang Z. Design and automated assembly of Planetary LEGO Brick for lunar *in-situ* construction. Autom Const 2020;118:103282.

[89] Mottaghi S, Benaroya H. Design of a lunar surface structure. I: design configuration and thermal analysis. J Aerosp Eng 2015;28:04014052.

[90] Meyers C, Toutanji H. Analysis of lunar-habitat structure using waterless concrete and tension glass fibers. J Aerosp Eng 2007;20:220–6.

[91] Malla RB, Chaudhuri D. Analysis of a 3D frame—membrane structure for lunar base. In: Proceedings of the 10th Biennial International Conference on Engineering, Construction, and Operations in Challenging Environments and Second NASA/ARO/ASCE Workshop on Granular Materials in Lunar and Martian Exploration; 2006 Mar 5–8; Houston, TX, USA. Washington, DC: American Society of Civil Engineers; 2006. p. 1–8.

[92] Straub J. In search of technology readiness level (TRL) 10. Aerosp Sci Technol 2015;46:312–20.

[93] Land P. Lunar base design. In: Lunar bases and space activities of the 21st century. Houston: Lunar and Planetary Institute; 1985. p. 363.

[94] Naser MZ. Extraterrestrial construction materials. Prog Mater Sci 2019;105:100577.

[95] Kessler P, Prater T, Nickens T, Harris D. Artemis deep space habitation: enabling a sustained human presence on the Moon and beyond. In: Proceedings of the 2022 IEEE Aerospace Conference (AERO); 2022 Mar 5–12; Big Sky, MA, USA. Reston: American Institute of Aeronautics and Astronautics; 2022. p. 1–12.

[96] Harris DW, Kessler PD, Nickens TM, Choate AJ, Horvath BL, Simon MA et al. Moon to Mars (M2M) habitation considerations: a snap shot as of January 2022. Technical Memorandum. Huntsville: NASA Marshall Space Flight Center; 2022. No. NASA/TM-20220000524.

[97] Flores G, Harris D, McCauley R, Canerday S, Ingram L, Herrmann N. Deep space habitation: establishing a sustainable human presence on the moon and beyond. In: Proceedings of the 2021 IEEE Aerospace Conference (50100); 2021 Mar 6–13; Big Sky, MA, USA. New York City: IEEE; 2021. p. 1–7.

[98] Woerner J. Moon Village: a vision for global cooperation and Space 4.0 [Internet]. Paris: European Space Agency; 2016 Dec 23 [cited 2024 Feb 9]. Available from: https://blogs.esa.int/janwoerner/2016/11/23/moon-village/.

[99] Inocente D, Koop C, Petrov GI, Hoffman JA, Sumini V, Makaya A et al. Master planning and space architecture for a moon village. In: Proceedings of the 70th International Astronautical Congress (IAC); 2019 Oct 21–25; Washington, DC, USA. Paris: International Astronautical Federation (IAF); 2019.

[100] Whitmore M, Boyer J, Holubec K. NASA-STD-3001, space flight human-system standard and the human integration design handbook. In: Proceedings of the Industrial and Systems Engineering Research Conference; 2012 May 19–23; Orlando, FL, USA. San Diego: INCOSE-International Council On Systems Engineering; 2012.

[101] Drysdale A. Esm history, capability, and methods. London: SAE International; 2003. SAE Technical Paper 2003-01-2630.

[102] Nagendra NP. System analysis and evaluation of greenhouse modules within Moon/Mars habitats. In: Proceedings of the 39th COSPAR Scientific Assembly; 2012 Jul 14–22; Mysore, India. Online: the SAO/NASA Astrophysics Data System; 2012.

[103] Farries KW, Visintin P, Smith ST, van Eyk P. Sintered or melted regolith for lunar construction: state-of-the-art review and future research directions. Constr Build Mater 2021;296:123627.

[104] China's Lunar and Deep Space Exploration. Notice on soliciting intentions for the development of scientific payloads and operational robots for the Chang'e-8 mission [Internet]. Beijing: China National Space Administration; 2024 Feb 7 [cited 2024 Feb 29]. Available from: http://www.clep.org.cn/n5982341/c10472114/content.html. 2024-02-07. Chinese.